Construction and Building Materials 158 (2018) 1–10

Contents lists available at ScienceDirect

Construction and Building Materials

journal homepage: www.elsevier.com/locate/conbuildmat

Effects of nanocharcoal coconut-shell ash on the physical and rheological properties of bitumen

Siti Nur Amiera Jeffry [a], Ramadhansyah Putra Jaya [a,*], Norhidayah Abdul Hassan [a], Haryati Yaacob [a], Jahangir Mirza [b,c], Siti Hasyyati Drahman [b]

[a] Faculty of Civil Engineering, Department of Geotechnics and Transportation, Universiti Teknologi Malaysia, 81310 UTM, Johor Bahru, Malaysia
[b] Faculty of Civil Engineering, Construction Research Centre, Institute for Smart Infrastructure and Innovative Construction (ISIIC), Universiti Teknologi Malaysia, 81310 UTM, Johor Bahru, Malaysia
[c] Department of Materials Science, Research Institute of Hydro-Québec, 1800 Mte. Ste. Julie, Varennes, Québec J3X 1S1 Canada

HIGHLIGHTS

- Nanocharcoal ash as bitumen modification has higher rutting resistance.
- Nanocharcoal ash has large surface area which increased the interfacial forces within the bitumen.
- Nanocharcoal ash enhanced the cohesion of the bitumen with improved the physical and rheological properties.

ARTICLE INFO

Article history:
Received 5 February 2017
Received in revised form 1 October 2017
Accepted 3 October 2017

Keywords:
Nano-sized
Coconut shell
Bitumen
Physical properties
Rheological properties

ABSTRACT

Bitumen properties which correspond to high resistance to traffic and temperature are the prime requirements in prolonging the pavement life. To achieve these requirements, nanoscale materials are considered as potential candidates to increase pavement life. Therefore, to fulfill the need for sustainable structures, this research focused on nanosized (1–100 nm) charcoal from coconut-shell waste as an additive in bitumen. Particle-size analysis and transmission electron microscopy indicated that 15 h of ball-mill grinding produced nanocharcoal ash (NCA) with an average size of 57.7 nm. Then, 0% (control), 1.5%, 3%, 4.5%, 6%, or 7.5% NCA by weight of bitumen PEN 60/70 was added. Penetration, softening point, viscosity, ductility, and dynamic shear rheometer (DSR) tests were performed to investigate the physical and rheological properties of the modified bitumen. Rolling thin film oven and pressure aging vessel tests were used to simulate the aging properties of the bitumen. Results showed that NCA decreased the penetration and increased the softening point of the bitumen, whereas viscosity increased with increased NCA percentage. High rutting and cracking resistance at failure temperatures of 76 and 22 °C, respectively, in the modified bitumen were revealed by the DSR test. Notably, 6% NCA was the optimum content that can improve rutting and cracking resistance.

1. Introduction

Good-quality pavement should exhibit high structural integrity, which provides a strong, smooth, and safe riding surface for road users. However, due to numerous factors, mainly traffic and temperature, asphalt pavements tend to become damaged, which decreases the serviceability, efficiency, and safety of asphalt pavement [1–3]. In Malaysia, rutting and fatigue cracking are the common types of distress in asphalt pavements. One of the factors that lead to pavement distress is the poor bitumen properties. Bitumen is a viscoelastic material that is easily affected by temperature. Inadequate physical properties, such as stiffness, sensitivity to temperature, and rheological properties (resistance to rutting and fatigue cracking) are the factors that contribute to this problem. Considerable research regarding asphalt modification is required for compliance with the current traffic loadings and high temperature to prolong the life of the pavement [1,4].

Nanoscale materials have recently been considered as potential candidates for increasing the life of pavement. The nanosized particles range from 1 nm to 100 nm in size [5–11]. Accordingly, nanomaterials exhibit higher reactivity compared with other common-sized particles because of their small size. The small size of particles leads to large surface area, which can increase exposure

* Corresponding author.
E-mail address: ramadhansyah@utm.my (R.P. Jaya).

https://doi.org/10.1016/j.conbuildmat.2017.10.019
0950-0618/

to collisions and the frequency of collisions. Hence, the rate of reaction will increase, leading to strong interfacial forces, which improve the bonding between materials. A workshop by the National Science Foundation in 2006 indicated that nanoscience and nanotechnology can lead to improvements in the asphalt pavement technology [11]. FHWA (2008) [7] expected that one of the long-term effects of using nanomaterials in the pavement research is to obtain novel pavement materials with high resistance to traffic and environment. Numerous studies have incorporated nanomaterials as bitumen modifier owing to their unique properties, which improve both the rheological and engineering properties of bitumen and mixtures [12]. Various types of nanomaterials, such as nanoclay, nanosilica, carbon nanofiber (CNF), and others, have been used to modify the asphalt binder. Jamshidi et al. [12] reported that nanoparticles can improve both the rheological and engineering properties of bitumen and mixtures. Khattak et al. [13] showed that CNF improves the viscoelastic response and rutting resistance of bitumen. Shafabakhsh and Ani [14] utilized nano-TiO_2 and nano-SiO_2 in bitumen, producing higher resistance against rutting through the dynamic shear rheometer (DSR) test. Zhang et al. [15] reported that nano-SiO_2, nano-TiO_2, and nano-ZnO decreased penetration and increased softening.

Previous studies on nanomaterials mostly utilized inorganic nanomaterials in the bitumen. One of the approaches to mitigate the risks of using hazardous nanomaterials on the environment, health, and safety is to replace these materials with an alternative [7]. Naturally sourced material is one such solution for this problem. Few studies that the incorporation of natural resource nanomaterials, such as palm oil fuel ash, rice husk ash, and rattan, in composite materials demonstrated that nanomaterials can enhance the properties and performances of materials [16–18].

Moreover, the production of nanomaterials from natural wastes can help to minimize the waste materials and fulfill the need of sustainable structures [1,19,20]. Among all waste materials, coconut shell is seen as the material with the most potential to be produced as nanomaterials because of its strength and good quality in various composite structures. Coconut shell is one of the agricultural wastes that are abundantly available and discharged by various industries [20–22] Coconut is the fourth crop in Malaysia after palm oil, rubber, and paddy, sequentially [23]. Coconut is an extremely strong, rigid, and lightweight material. In addition, the material is environmentally friendly because of its biodegradability and emission of a relatively low amount of carbon dioxide when burned [24]. Therefore, this paper focuses on the utilization of nanocharcoal ash (NCA) from coconut shell as the bitumen modifier and its effects on bitumen performance. Penetration, softening point, viscosity, and dynamic shear rheometer (DSR) tests were performed to investigate the effects of nanosized charcoal on the physical and rheological properties of bitumen.

2. Materials and method

2.1. Asphalt binder

The bitumen PEN 60/70 from Chevron, Malaysia was used. Table 1 shows its physical properties.

2.2. Preparation of nanomaterial

Each 200 g of coconut shell was burnt in a furnace (42 × 53 × 55 cm^3) at 450 °C for 5 min. This temperature was selected based on the thermal properties of charcoal [25–27]. Charcoal was then produced and crushed using the Los Angeles abrasion machine to produce finer sizes. The fine charcoal was subsequently sieved to obtain the particle sizes of less than 75 μm. The material was ground using a ball mill to obtain nanosized charcoal. A total of 56 steel balls of different diameters were used as grinding media. Table 2 shows the specification of the grinding media. The different grinding times were 5, 10, 15, and 20 h. A total of 100 g of material was fed into the ball mill for each grinding time. Particle-size analysis (PSA) and transmission electron microscopy (TEM) were carried out on the ground samples to check the size.

Table 1
Physical properties of PEN bitumen 60/70.

Specific gravity	1.03
Penetration at 25 °C (dmm)	60.9
Softening point (°C)	49.0
Viscosity at 135 °C (Pa·s)	0.5

Table 2
Grinding balls.

Diameter (mm)	Weight (g)	Amount
25	407.2	7
20	513.8	17
16	252.5	17
12	97.1	15

2.2.1. Particle-size analysis (PSA)

The average particle size of ground samples, which were processed for 5, 10, 15, and 20 h, was analyzed by a PSA Malvern Zeta-sizer Nano-ZSP ZEN5600. PSA was used to obtain the average size from the peak of particle-size distribution of the sample. Dynamic light scattering technique was used in this test, in which the samples were prepared by using a wet process. This technique can be used to measure the particle and molecular sizes ranging from 0.3 nm to 10 μm.

2.2.2. Transmission electron microscopy (TEM)

TEM Hitachi HT7700 was used to visualize and analyze the nanocharcoal. This instrument can be used to measure the sample in the microscale (1 μm) to nanoscale (1 nm). TEM can analyze the sample with high-image resolution and magnification.

2.3. Bitumen modification

2.3.1. Modification using different particle sizes of charcoal

5, 10, 15, and 20 h ground samples (6% by weight of bitumen) were added in the bitumen PEN 60/70. The percentage was selected to examine the effects of the same amount of material with different particle sizes in asphalt binder. Moreover, 6% was selected for the study of the high effects of particles with and without nanosized charcoal in the bitumen.

2.3.2. Nanocharcoal ash (NCA) modified bitumen

NCA with amounts of 1.5%, 3%, 4.5%, 6% and 7.5% were added by weight of bitumen PEN 60/70. These percentages were selected based on the analysis of previous studies [12,14,28,29]. The 1.5% gap was selected to examine the sensitivity of the NCA content in the bitumen.

2.3.3. Blending process

The blending process was conducted by using a high shear mixer at 1500 rpm at 160 °C for 60 min. A speed of 1500 rpm was used to ensure that the additives were dispersed well in the bitumen. Blending was conducted at 160 °C because considerably high temperature level can cause the aging of bitumen. Approximately 60 min of mixing was used to ensure adequate mixing

between the additive and bitumen to produce a homogenous binder [11].

2.3.4. Storage stability test

Storage stability test for modified bitumen was carried out in accordance with ASTM D5976 [30] to evaluate the stability of the NCA at high temperatures prior to physical properties tests. About 50 g of the modified bitumen was poured into an aluminum tube (25 mm × 140 mm) after blending for each percentage. The modified samples were then heated in the oven for 2 days at temperature of 163 °C. After that, the heated samples were placed in the freezer at −6.3 °C for 4 h in order to turn the liquid form of the bitumen into solid. The sample was cut into 3 equal parts after being removed from the freezer. The softening point of the top and bottom parts of the bitumen was then tested. The difference between the top and bottom parts should not more than 2.2 °C.

2.4. Bitumen property test

2.4.1. Penetration test

The consistency of bitumen was measured by penetration test according to the ASTM D5/D5M-3 standard [31]. This test is the simplest approach to obtain the penetration value of the bitumen. A low penetration value indicates the hardness of the bitumen. The bitumen was heated and poured into a penetration cup prior to testing. The sample was then placed into a water bath for 1 h at 25 °C after cooling. The penetration equipment was used to perform the test with the applied total load of 100 g for 5 s at 25 °C.

2.4.2. Softening point test

The softening point test was conducted according to ASTM D36/D36M−14e1 [32]. This test is important because it determines the temperature susceptibility of the bitumen. The bitumen was heated and poured into two rings and cooled for 30 min. The two rings and two ball centering guides were placed on the ring holder in a liquid bath. Subsequently, 3.5 g of steel balls were placed on each sample and heated. The temperature at which the bitumen touched the base plate was recorded, and the mean temperature of the two samples was calculated.

2.4.3. Viscosity test

Viscosity test was conducted to determine the resistance of asphalt binder to flow. A rotational viscometer was used to conduct the test according to ASTM D4402 [33] at 135 and 165 °C. A Brookfield viscometer and a Thermosel system were used to determine rotational viscosity. A cylindrical spindle size number 27 was immersed in the asphalt binder at constant temperature, and the torque that maintained a constant rotational speed of 20 rpm of the spindle was determined. This torque is related to the viscosity of the binder. The viscosity test is important to evaluate the workability of the asphalt binder in terms of pumping and mixing at high construction temperature. Given the asphalt binder performance, the low viscosity of asphalt binder will lead to rutting or flushing at high temperature. Moreover, high viscosity will cause non-load cracking at low temperature. Therefore, a suitable viscosity grade must be determined to satisfy the climatic conditions.

2.4.4. Penetration index (PI) and penetration–viscosity number (PVN)

The relationship between the penetration–softening point value and penetration viscosity value can be expressed in terms of PI and PVN, as shown in Eqs. (1) and (2), respectively [1]. These indicators were used to measure the temperature susceptibility of the bitumen:

$$\mathrm{PI} = \frac{(1951.4 - 500\log P - 20SP)}{(50\log P - SP - 120.14)} \quad (1)$$

$$\mathrm{PVN} = -1.5\left(\frac{(4.258 - 0.7967\log P - \log V)}{(0.795 - 0.1858\log P)}\right) \quad (2)$$

where P is penetration value (dmm), SP is softening point value (°C) and V is viscosity (Pa·s).

2.4.5. Ductility test

Ductility test was used to characterize the cracking of the bitumen at low temperature. This test is also used to determine the cohesiveness of the bitumen. Ductility testing was carried out in accordance with ASTM D113-07 [34]. The bitumen was tested at 25 °C in a water bath and pulled apart at the rate of 5 cm/minute until the bitumen breaks. The specific gravity of the water was adjusted to the same specific gravity of the bitumen. The length of the bitumen stretch prior to break was then recorded.

2.4.6. Dynamic shear rheometer (DSR)

A DSR was used to measure the rheological properties of bitumen. This test was conducted in accordance with ASTM D7175-15 [35]. The viscoelastic behavior of bitumen was determined by the complex shear modulus G^* and phase angle δ at intermediate to high temperature. G^* and δ values depend on the test temperature and frequency of loading. The rutting (December 2016-January 2017) and fatigue cracking (May-June 2017) performances of the asphalt pavements were analyzed from $G^*/\sin\delta$ and $G^*.\sin\delta$ respectively. In this study, the test was conducted from 46 °C to 82 °C at an increment of 6 °C for the rutting performance and 40–22 °C at a decrement of 3 °C for the fatigue cracking performance. For the unaged and RTFO samples, a 1 mm-thick plate and 25 mm-diameter top plate was used. Meanwhile, 2 mm-thick plate and 8 mm-diameter top plate were used for PAV sample. The bitumen sample was sandwiched between two fixed plates. Stress was applied on top of the sample by the oscillating top plate, which oscillated at 1.59 Hz, to measure the maximum stress, maximum strain, and time lag of stress and strain.

2.4.7. Rolling thin film oven (RTFO)

The rolling thin film oven (RTFO) was used to simulate short-term aging of bitumen and aging of the bitumen during the mixing and compaction of the hot mix asphalt at the field. This test was carried out according to the ASTM D2872-12e1 [36]. Eight RTFO bottles were poured with 35 g of bitumen each. Then, the bottles were placed in the rotating carriage in an oven heated to 163 °C. The carriages were then rotated at 15 rpm for 85 min with the airflow into each bottle at 4000 mL/min. The mass loss before and after aging condition of the bitumen was recorded. The residue from the bottles was transferred in the container for DSR testing.

2.4.8. Pressure aging vessel (PAV)

PAV testing was carried out in accordance with ASTM D6521-13 [37]. PAV was used to simulate the long-term aging of bitumen during the asphalt pavement service life. The RTFO sample, which was used to form the PAV sample, was heated, and approximately 50 g was poured in a pan. Ten pans were used to age the RTFO samples. A rack comprising the pans was then placed in the PAV. After preheating, the PAV was operated at 2.1 MPa pressure and 100 °C temperature for 20 h. The PAV samples were then heated at 163 °C in an oven for 30 min to release entrapped air. Then, the samples were further tested using DSR.

3. Results and discussion

3.1. PSA

Fig. 1 shows the cumulative particle-size distributions of charcoal ash ground for 5, 10, 15, and 20 h. The particle size of charcoal

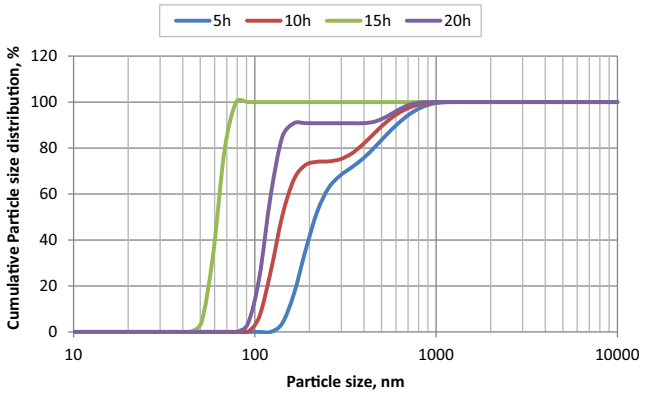

Fig. 1. Cumulative particle size distribution of ground charcoal.

ash decreased with grinding time from 5 h to 15 h. Particle size then increased when the ash was subjected to 20 h grinding time. The highest particle sizes produced for each grinding time were 164.2 (18.8%), 122.4 (24.2%), 58.77 (45.8%), and 105.7 nm (36.2%) after grinding times of 5, 10, 15, and 20 h, respectively. Correspondingly, the average particle sizes were 282.7, 211, 57.7, and 149.2 nm. These results showed that 15 h grinding time contributed a substantial nanoparticle size (57.7 nm) range, whereas the particle sizes obtained for the other grinding times exceeded 100 nm. According to Hornyak et al. [38], the novel and distinct properties of materials were developed at the nanoscale of 1–100 nm. In addition, the particle size continued to decrease and increase again until a certain limit. Austin and Bagga [39] reported that high grinding times yield no fine sizes even with the same mill power. This condition is caused by the decreased particle breakage rate, agglomeration, and longer time than the optimum grinding time. According to Austin and Bagga [39], the particles are difficult to break when the ball falls onto a bed of particles, which becomes powder because the particles tend to move away from the balls. Furthermore, the powder bed only absorbs the impact without breaking the particles, thereby reducing the rate of particle breakage. Fine particles also possess large surface areas, which tend to agglomerate because of the increased interparticle forces and influence by the air. Thus, the optimum grinding time to obtain the nanocharcoal ash (NCA) in this study was 15 h, yielding an average particle size of 57.7 nm.

3.2. TEM

TEM was performed on 15 h ground charcoal to confirm the shape and size through high-resolution images, as shown in Fig. 2. The particle size of materials shown in the images also included the shape of the grid used during sample preparation. Fig. 2(a) shows the particle sizes of the ground charcoal at the scale of 100 nm. According to Fig. 2(b), the particle size ranged from 19 nm to 50 nm, respectively. In addition, the particle size showed a sphere and crushed shape, with all three dimensions within the range of 1–100 nm. The images also present different shades because of particle overlap, which darkened certain parts of the particles. The term NCA was used to denote the nanomaterial in this research. Table 3 presents the properties of NCA. The nanosized particles showed larger surface area than those of other materials. This property can help increase the bonding of the materials and the bitumen.

3.3. Bitumen modified with different particle sizes of charcoal

Table 4 shows the 5, 10, 15, and 20 h ground charcoals, which were designated as MC1, MC2, NCA, and MC3, respectively, based on the particle size obtained from PSA.

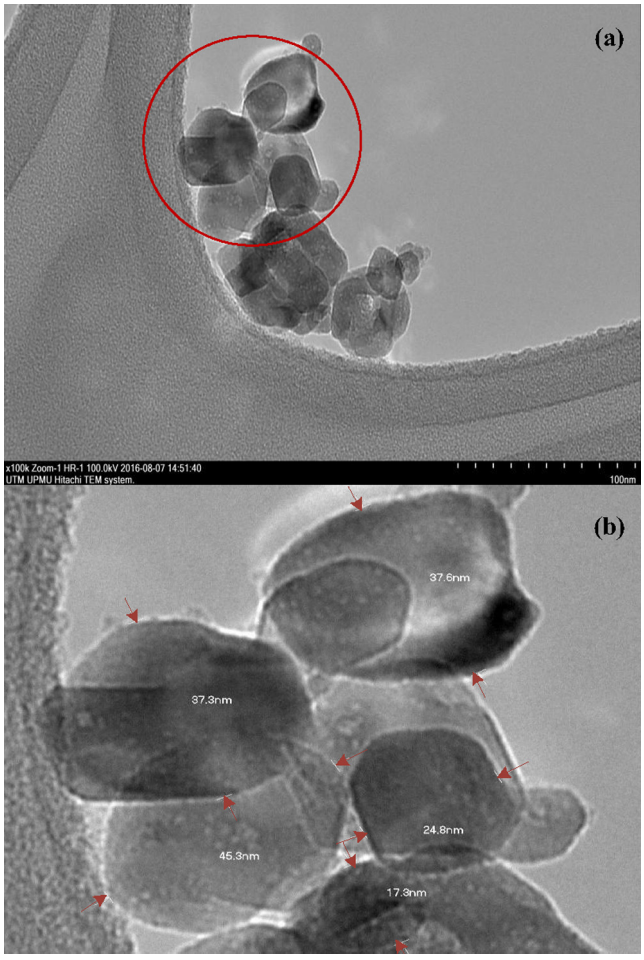

Fig. 2. TEM of 15 h ground charcoal (NCA): a) Particle sizes at 100 nm scale; b) Range of particle sizes in the red circle. (For interpretation of the references to colour in this figure legend, the reader is referred to the web version of this article.)

Table 3
Properties of nanocharcoal coconut shell.

Properties	Content
Average size (nm)	57.7
Specific surface area (m^2/g)	112.74
Phase	Black powder
Elemental analysis (%)	C = 77.4
	H = 2.7
	N = 0.24
	S = 0.13
	O = 19.5

Table 4
Ground samples from PSA used in bitumen.

Grinding time (hour)	Size		Sample designated
	Nm	μm	
0	–	–	Control
5	282.7 > 100	0.3	Micro charcoal 1 (MC1)
10	211.0 > 100	0.2	Micro charcoal 2 (MC2)
15	57.7 < 100	0.06	Nanocharcoal ash (NCA)
20	149.2 > 100	0.15	Micro charcoal 3 (MC3)

Table 5 shows the results of the penetration, softening point, and viscosity tests of the modified bitumen. The penetration values of the modified bitumen markedly decreased with increased softening points compared with those of the control bitumen. The

Table 5
Physical properties of modified bitumen in samples with different particle sizes.

Designated	Penetration (dmm)	Softening point (°C)	PI	Viscosity (Pa·s)		PVN
				135 °C	165 °C	
Control	60.9	49.0	−1.0	0.5	0.2	-0.4
MC1	41.7	50.8	−1.4	0.6	0.2	-0.6
MC2	44.9	51.0	−1.2	0.7	0.3	-0.3
MC3	44.5	51.0	−1.2	0.63	0.2	-0.4
NCA	45.2	52.0	−0.9	0.7	0.3	-0.3

decrease in penetration values indicates that the bitumen was stiffer than the control bitumen. The penetration values of modified bitumen were decreased by 31.5%, 26.3%, 26.9%, and 25.8% respectively, whereas the softening points were increased by 3.7%, 4.1%, 4.1%, and 6.1% for MC1, MC2, MC3, and NCA respectively. The PI range for the modified bitumen was out of the construction PI range, that is, −1 to +1, except for the NCA-modified bitumen, which presented a PI of −0.9. The viscosities of the modified bitumen were 0.6, 0.7, 0.63, and 0.7 Pa·s for MC1, MC2, MC3, and NCA respectively; these values were higher than the 0.5 Pa s of the control sample. The viscosity was reduced as the temperature increased to 165 °C. The PVN of the NCA-modified bitumen was −0.3 lower than that of the control sample.

Based on the results, no significant differences were observed among MC1-, MC2-, and MC3-modified bitumen because the gap between the particle sizes was extremely small, as shown in Table 5. Meanwhile, the NCA presented novel properties at the nanosize, which differed from particles without the nanosized features. Despite the slightly lower penetration values of MC1, MC2, and MC3 compared with that of NCA, the PI of NCA sample was in the range and higher than that of the MC samples because of slightly higher softening point. The micro-sized samples affect penetration owing to the lower stability and inhomogeneity of the modified bitumen. The micro particles did not disperse well owing to their larger particle size, leading to non-uniformity of the blended bitumen. Thus, the needle penetrates at the surface where the particles accumulated, producing stiffer bitumen. However, this action will not produce long-term effects to the bitumen because of the inhomogeneity. Furthermore, penetration test is only a consistency test conducted at ambient temperature only (25 °C), and the samples were not subjected to traffic and environmental conditions.

On the other hand, the nanosized particles are dispersed well in the bitumen, creating strong bonding with the bitumen. Thus, a homogenous bitumen state was formed. The associations of NCA and the bitumen increased the cohesiveness of the bitumen, leading to high viscosity. High viscosity is important because it is less easily influenced by high temperature and results in high resistance to rutting in rheological performance. However, larger size particles do not disperse well in the bitumen but still form high bitumen viscosity. The effects on rheological performance can be seen when the rutting resistances of the MC1, MC2, and MC3 were lower than that of NCA.

Fig. 3 shows the rutting performance of the control and modified bitumen. The modified samples can resist rutting until 70 °C prior to failure at 76 °C. Modified bitumen exhibited better performance than control sample, which resisted rutting until 64 °C and failed at temperature of 70 °C. NCA showed the most notable performance in rutting resistance. In the range of 58 °C–76 °C, $G^*/\sin\delta$ was higher than those of other samples, and the rutting resistance was 1709 Pa at 70 °C prior to failure by 996.5 Pa at 76 °C. Based on this test, effects of the NCA in bitumen can be noticed clearly compared with physical properties tests. The high dispersion of NCA in the bitumen leads to high bonding between the NCA and the bitumen, enhancing the rutting resistance at high temperature. Given

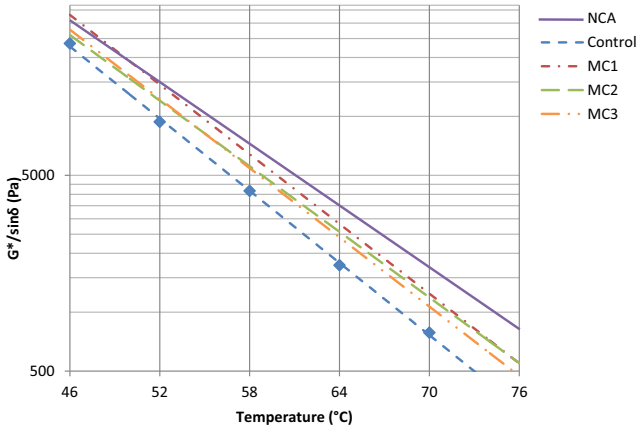

Fig. 3. Rutting performance of bitumen modified with different particle sizes.

the small gap of the average particle size among MC1, MC2, and MC3 samples, the samples showed no significant differences in the rutting parameter. NCA increased the rutting resistance relative to that of MC.

3.4. NCA-modified bitumen

NCA contents of 0% (control sample), 1.5%, 3%, 4.5%, 6%, and 7.5% were added to bitumen PEN 60/70. These percentages were selected to examine the sensitivity of NCA content in the bitumen and to obtain the optimum NCA content in bitumen. In this section, the stability of the unaged modified bitumen was presented. Subsequently, the unaged and RTFO-aged modified samples were subjected to penetration, softening point, viscosity, and DSR tests. Further test using DSR was carried out to examine the fatigue cracking of the sample simulated by PAV.

3.4.1. Storage stability test

The difference between the top and bottom part of the modified bitumen was less than 2.2 °C as shown in Table 6. This indicates that the blend of NCA and the bitumen are well dispersed and still in the stable and homogenous state even though placed at high temperature conditions. The compatibility between the NCA and bitumen also showed that the method used to blend the materials was adequate. High surface area of the NCA leads to the strong interfacial forces between the surface of the NCA and the bitumen. Thus, the dispersion of the NCA in the bitumen was improved.

3.4.2. Penetration test

Fig. 4 shows the penetration test results of unaged and RTFO-aged modified samples. For the unaged samples, the modified bitumen showed improved penetration compared with the control sample at 60.9 dmm. Penetration was reduced approximately by 19.4%, 22.5%, 23.5%, 25.8%, and 24.3% compared with the control sample for 1.5%, 3%, 4.5%, 6%, and 7.5% NCA samples, respectively. The 6% NCA sample displayed a higher percentage of improvement

Table 6
Storage stability test of modified bitumen.

NCA (%)	Diff. top and bottom parts (°C)	Specification <2.2 °C
1.5	0.5	Pass
3.0	0.2	Pass
4.5	0.7	Pass
6.0	0.4	Pass
7.5	0.2	Pass

than those of other samples with penetration value of 45.2 dmm. A low penetration value indicates that the bitumen is stiff and hard. In this research, NCA enhanced the stiffness of the bitumen. High stiffness leads to low susceptibility to high temperature. The penetration value was acceptable because all values exceeded 30 dmm. According to Brown [1], bitumen exhibits high resistance to cracking when the penetration exceeds 30 dmm with proper mixing design and compaction. NCA stiffened the bitumen, but not to the maximum level that can lead to cracking. The high surface area of NCA increased the bonding between NCA and the bitumen. Hence, the NCA properly enhanced the stiffness of the bitumen.

As expected, the penetration value for the RTFO-aged samples was lower than those of the unaged samples. A decreasing trend was observed for the samples with increased NCA content increased up to 6% NCA. The penetration values increased again at 7.5% NCA. The penetration of modified bitumen improved by 9.5%, 6%, 20.6%, 24.4%, and 19.9% compared with the control sample for 1.5%, 3%, 4.5%, 6%, and 7.5% NCA, respectively. The 6% NCA exhibited the highest stiffness of 23.9 dmm of all samples similar to the unaged samples. In addition, the increased penetration values of 7.5% for both unaged and aged samples were due to excessive NCA content; the excess amount of NCA did not bond with the bitumen matrix, leading to agglomeration. Hence, when the optimum content is reached, further addition of NCA will have no significant effect on the bitumen.

3.4.3. Softening point test

Fig. 5 shows the softening point values of modified bitumen for the unaged and RTFO-aged samples. For the unaged samples, the softening point values increased with increased NCA content. Both of the unaged and RTFO-aged samples showed increasing trends in softening point. The trend increased to approximately 3% NCA and showed no significant effect until 6% NCA was reached; then, the values started to be consistent until 7.5% NCA. The softening point of the control sample was 49 °C, which was lower than those of the modified samples of 1.5% (50.5 °C), 3% (51 °C), 4.5% (51 °C), 6% (52 °C), and 7.5% (52 °C) NCA. A high softening point indicates that the bitumen can withstand a certain level of temperature until the phase changes from solid to liquid. According to these results, the temperature at which the bitumen softened was high owing to strong particle forces between the NCA and the bitumen and increases the bonding between the particles. This shows that the bitumen exhibited low susceptibility to temperature.

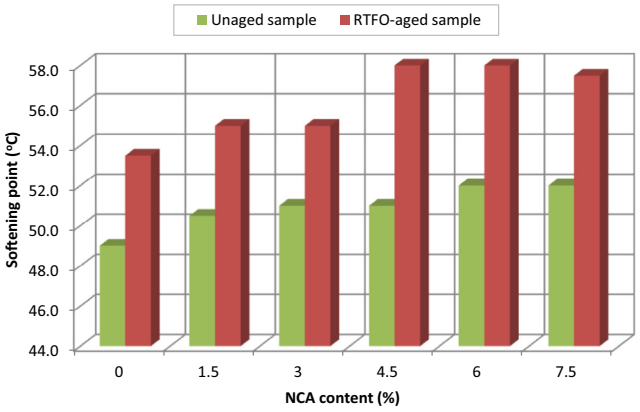

Fig. 5. Softening points of unaged and RTFO-aged samples.

Meanwhile, the softening points of the aged samples were higher than those of the unaged samples. The trend increased until 6% NCA and decreased at 7.5% NCA. The softening point of the control sample was 53.5 °C, which was lower than those of the modified samples. The values increased to 55 °C for both the 1.5% and 3% NCA and increased to 58 °C for 4.5% and 6% NCA prior to a decrease at 57.5 °C for 7.5% NCA. Although the percentage improvement between NCA contents showed no large differences, the last three percentages, namely, 4.5%, 6%, and 7.5% NCA, presented excellent results compared with those of the control sample. However, the penetration and softening point tests were not sufficient to validate the effects of NCA in the bitumen because the penetration test was only performed at only 25 °C, and the softening point test was subjected to one load only. Therefore, other performance tests are necessary to analyze the effects of NCA in bitumen.

3.4.4. Viscosity

The viscosity results at 135 and 165 °C for unaged and RTFO-aged modified bitumen, respectively, are shown in Fig. 6. The viscosity of the unaged modified bitumen at 135 °C was higher than that of the control sample. The viscosity of the control sample was 0.5 Pa s and increased to 0.6 Pa·s for 1.5% NCA. At 3%, 4.5%, and 6% NCA, the viscosity remained the same at 0.7 Pa·s. Subsequently, the viscosity started to increase again at 7.5% NCA to 0.87 Pa·s. When the test was conducted at 165 °C, the viscosity of

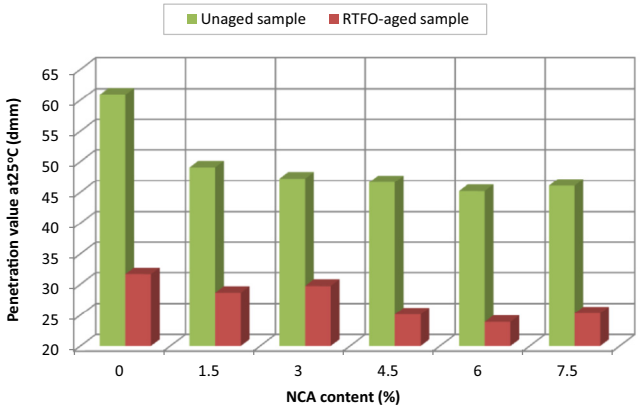

Fig. 4. Penetration values of unaged and RTFO-aged samples.

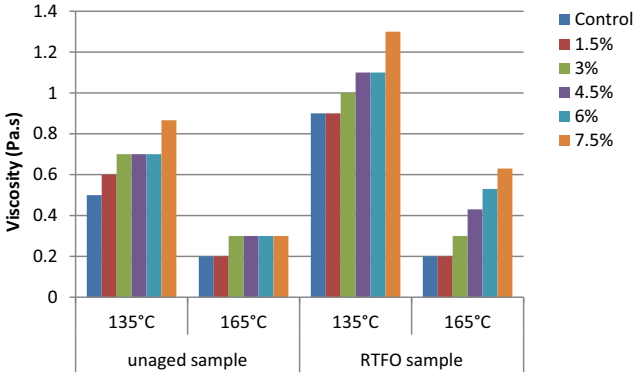

Fig. 6. Viscosity values for unaged and RTFO-aged samples.

the samples decreased. The viscosity of the control sample was 0.2 Pa·s, which was the same as that of the 1.5% NCA. At 3%, the viscosity increased to 0.3 Pa·s and remained constant for 4.5%, 6%, and 7.5% NCA.

For the aged sample, the viscosity was evidently higher than that of the unaged sample. At 135 °C, the viscosity of the control sample was 0.9 Pa·s, which was similar to that of 1.5% NCA. The viscosity increased to 1.0, 1.1, 1.1, and 1.3 Pa·s for 3%, 4.5%, 6%, and 7.5% NCA, respectively. At 165 °C, the viscosity of the control sample and 1.5% NCA was 0.2 Pa·s. The viscosity increased to 0.3 Pa·s for 3% NCA and constantly increased for 4.5%, 6%, and 7.5% NCA with viscosity values of 0.43, 0.53, and 0.63 Pa s, respectively.

Based on this analysis, the viscosity of modified bitumen for both unaged and aged samples was less than 3 Pa·s. The addition of 1.5% NCA to the bitumen exerted no significant effect because nearly all viscosity values remained almost the same as that of control sample. NCA started to take effect at 3% and remained constant until 6% before starting to increase again at 7.5%. This showed that NCA has high adhesion with bitumen. It was also observed that even though 7.5% NCA has the highest resistance to flow due to its high viscosity for both unaged and aged samples but its viscosity was considerably high, which does not seem to be economically beneficial. High bitumen viscosity presents both advantages and disadvantages. In this research study, the addition of NCA in the asphalt binder increased the viscosity. The high viscosity of bitumen increased the mixing and compaction temperature as well as the construction costs. However, the high cohesion of the bitumen increased the adhesion between the bitumen and the aggregates, thereby enhancing the performance of the pavement. Hence, the optimum NCA content should be selected by considering the properties of bitumen and its cost.

3.4.5. Temperature susceptibility

Table 7 displays the PI and PVN of the unaged and aged NCA. Brown et al. [1] indicated that the suitable PI for road construction was between −1 and +1. On one hand, a low PI value, approaching the negative which is less than −1, means that the sample is highly susceptible to low temperature and can lead to cracking. On the other hand, a high PI value, approaching the positive which is more than +1, indicates low susceptibility at high temperature and can result in high resistance to permanent deformation or rutting. The PI for the unaged modified samples was lower than that of control sample. The PI for 4.5%, 6%, and 7.5% NCA ranged from −1 to +1. By contrast, the PI of the control sample for the aged condition decreased to −1.3 and was lower than that of the unaged sample, that is, −0.7. The modified samples showed increased PI, except for 1.5% and 7.5% NCA, which remained the same as those of the unaged condition. The PI of the modified samples was higher than that of the control sample under the unaged condition and lower PI under the aged condition. In addition, the unaged NCA obtained a lower PVN than that of the control sample. The aged NCA also showed low PVN values compared with that of the control sample, except for 1.5% NCA. Brown et al. [1] reported that the range of PVN for bitumen was between +0.5 and −2.0. A low PVN value indicates high-temperature susceptibility. The NCA can improve the bitumen by reducing the temperature susceptibility to lower than that of the control bitumen. Moreover, no difference was observed, except for the control sample and the 7.5% NCA between the unaged and aged NCA. This result can be due to PVN which remained unchanged even after aging. By contrast, the PI will change during short-term and long-term aging [1].

Table 7
PI and PVN of modified bitumen.

NCA (%)	Unaged		RTFO-aged	
	PI	PVN	PI	PVN
0	−0.7	−0.4	−1.3	−0.3
1.5	−1.2	−0.4	−1.2	−0.4
3.0	−1.2	−0.2	−1.1	−0.2
4.5	−1.0	−0.2	−0.8	−0.2
6.0	−1.0	−0.3	−0.9	−0.3
7.5	−0.9	0.02	−0.9	−0.07

3.4.6. Ductility test

Fig. 7 shows the ductility results of the control and modified bitumen. Decreasing trends were observed with increased NCA content. The ductility of the modified bitumen was lower than that of the control bitumen by 28%, 32%, 38%, 46%, and 49% for 1.5%, 3%, 4.5%, 6%, and 7.5% NCA, respectively. These results showed that the modified bitumen tend to crack due to the bitumen elongation, which was decreased as the NCA content increased. However, the cohesion of the bitumen was improved, thus enhancing the rutting performance. Low ductility of the bitumen indicated stiff and hard to stretch because of the high cohesion of the bitumen. Due to the high surface area of NCA, strong particle bonding was formed between the NCA and the bitumen matrix. Thus, cohesion in the bitumen increases. Given that thicker bitumen was produced, the bitumen is more difficult to elongate and break faster than the thinner bitumen, which elongates more.

3.4.7. Rutting performance ($G^*/\sin\delta$)

Fig. 8 shows the DSR results for the unaged samples of NCA. The performance grade of the control sample was 64 °C prior to failure at 70 °C. Meanwhile, the modified samples can resist rutting until 70 °C prior to failure at 76 °C. The rutting parameter ($G^*/\sin\delta$) of

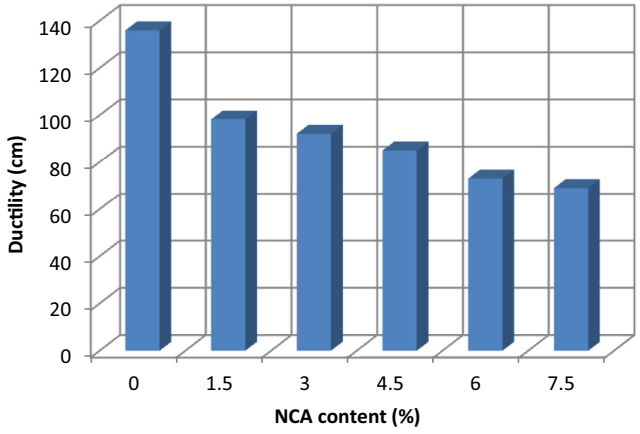

Fig. 7. Ductility values versus different NCA contents.

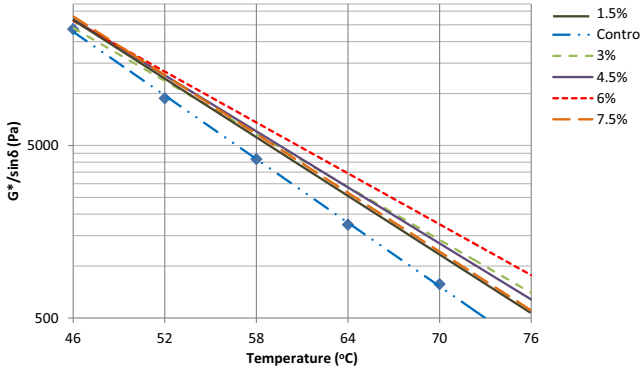

Fig. 8. Rutting performance of NCA under unaged condition.

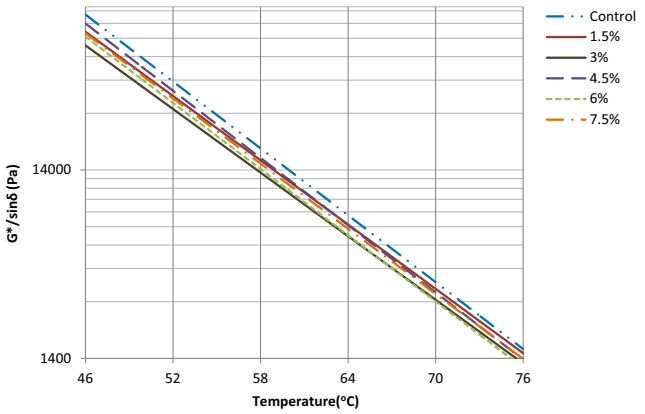

Fig. 9. Rutting performance of NCA at short-term aging condition.

the modified samples was higher than that of the control sample. The $G^*/\sin\delta$ values recorded at 70 °C for 1.5%, 3%, 4.5%, 6%, and 7.5% NCA were 1327, 1333, 1497, 1709, and 1280 Pa, respectively. The most outstanding value of rutting resistance was observed with 6% NCA. High rutting parameter was observed at 52 °C until failure temperature. The rutting resistance increased as the NCA content increased up to 6% NCA, followed by a decrease at 7.5% NCA. This finding indicated that an optimum NCA content of 6% was reached. Analysis showed that the NCA increased the stiffness of the control bitumen. The high surface area of the nanosized particles established strong interfacial forces between the particles of NCA and the bitumen. The particles reinforced the bitumen by increasing the bond and improving the cohesion of the bitumen. Subsequently, the bitumen properties were enhanced, thereby increasing the stiffness and improving rutting performance.

The RTFO samples shown in Fig. 9 demonstrate that both the control and modified samples resisted rutting until 70 °C before failing at 76 °C. After short-term aging, all the samples evidently became markedly stiff, thereby increasing the rutting resistance. The control sample showed higher performance than modified samples at approximately all temperatures; this result was contradictory to those of unaged NCA. The rutting resistance values of the control sample at 70 °C were 3341 and 1767 Pa at a failure temperature of 76 °C, which were the highest of all modified samples. Besides, rutting performance showed no significant differences between the NCA contents. The 6% NCA obtained the lowest rutting parameters at 70 and 76 °C with $G^*/\sin\delta$ of 2805 and 1417 Pa, respectively. The control sample exhibited a higher stiffness than the NCA samples during short-term aging. Excessively stiff bitumen at this stage can lead to higher stiffness during the service life of the pavement, which is not beneficial because fatigue cracking can occur.

These results showed that NCA retarded the aging process of the bitumen during the mixing and compaction stages, where the particles of NCA reduce the oxidation process by distributing the heat in the bitumen. The large surface area of the NCA absorbs and distributes the heat rapidly relative to the control bitumen, which stands alone in distributing the heat in the slow rate and causing the bitumen to age quickly. Thus, 6% NCA was the optimum content that can retard the aging of the bitumen at higher temperature compared with other NCA contents.

3.4.8. Fatigue cracking performance ($G^*\cdot\sin\delta$)

Fig. 10 presents the fatigue cracking performance of the NCA-modified samples under the PAV condition. The increasing trend of the graph indicated that the modified samples resist fatigue cracking from intermediate to lower temperature. The failure temperature was reached when the fatigue cracking parameter ($G^*\cdot\sin\delta$) exceeded 5×10^6 Pa [1,34]. Apparently, 1.5%, 3%, and 4.5% NCA exhibited $G^*\cdot\sin\delta$ values of 5.144×10^6, 5.254×10^6, and 5.755×10^6 Pa, which are higher than that of the control sample which failed at temperature of 25 °C. Besides, no significant difference was found between the $G^*\cdot\sin\delta$ values of 1.5% and 3% NCA. The failure temperature of the control sample was at 22 °C, with $G^*\cdot\sin\delta$ of 7.206×10^6 Pa. Similar failure temperature was observed in 6% and 7.5% NCA, with the recorded $G^*\cdot\sin\delta$ values of 7.044×10^6 and 6.439×10^6 Pa, respectively. The optimum was reached because 6% and 7.5% NCA showed lower $G^*\cdot\sin\delta$ than the control sample. From this result, the 6% and 7.5% NCA exhibits higher resistance to fatigue cracking compared with other NCA contents. This finding showed that the 6% and 7.5% NCA can retard aging during the service life of the pavement compared with the 1.5%, 3%, and 4.5% NCA.

The presence of NCA in the bitumen increased the stiffness of the bitumen owing to strong bonding created between the NCA and the bitumen. This bonding leads to high cohesion and stiffer

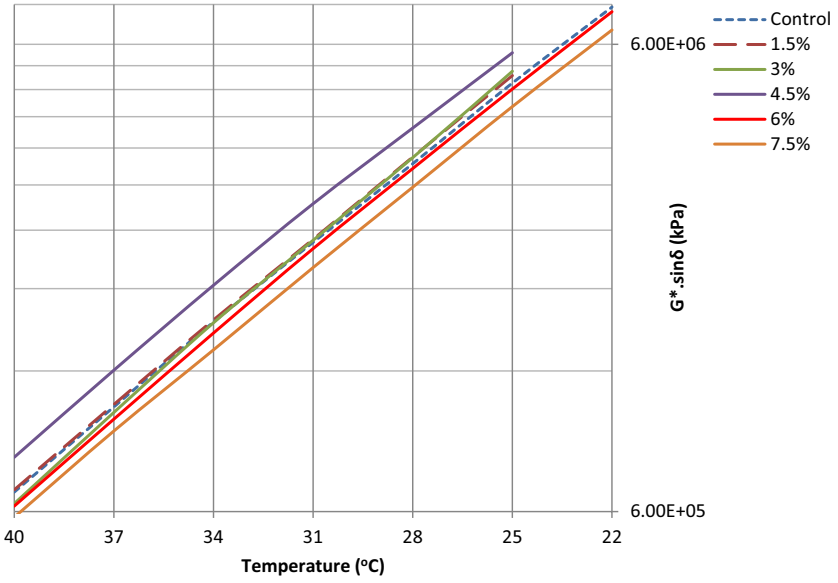

Fig. 10. Fatigue cracking performance of NCA under long-term aging condition.

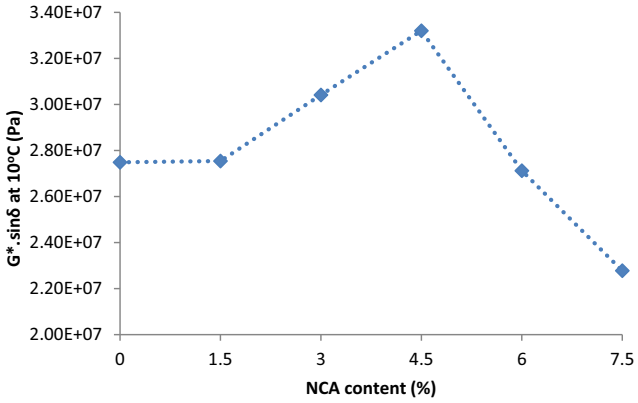

Fig. 11. Fatigue cracking parameter ($G^*\cdot\sin\delta$) at 10 °C.

bitumen than those of the control. However, during the service life of the pavement, bitumen tends to stiffen due to oxidation, leading to fatigue cracking. In this study, the absorbed heat in the NCA-modified bitumen during high temperature was stored longer than that in the control sample. Thus, during the decrement of test temperature, the NCA slowly released the heat and the heat loss under equilibrium condition, which helps in maintaining the viscoelasticity of the bitumen, instead of rapidly releasing the heat and stiffen the bitumen. A higher content of NCA, namely, 6% and 7.5%, can retard the aging process effectively compared with 1.5%, 3%, and 4.5% NCA sample due to particles of NCA accumulated more on the surface than distribute homogenously to release the heat. The large surface area of the NCA delayed the heat loss especially when more amounts were added. With the viscoelasticity of the bitumen and capacity of the bitumen to resist rutting and cracking under consideration, 6% NCA was considered as the optimum content in the bitumen because of its superior performance than that of the control bitumen.

The fatigue cracking parameter of the modified bitumen was investigated at a low temperature of 10 °C, as shown in Fig. 11. A similar trend was observed in this graph, in which the $G^*\cdot\sin\delta$ values of the 6% and 7.5% NCA were lower than that of the control bitumen. This finding shows that the NCA delayed the aging process of the bitumen even at 10 °C. This experiment shows that the cracking potential of the modified bitumen was lower than that of the control bitumen even at low temperature.

In addition, the ability of NCA to retard the aging was verified by conducting rutting test on PAV samples. Since this test was carried out according to RTFO specification, the rutting performance of the PAV sample was conducted until the $G^*/\sin\delta$ was less than 2.2 kPa.

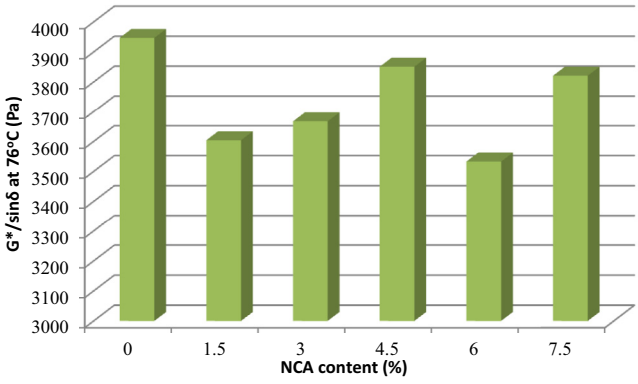

Fig. 12. Rutting parameter ($G^*/\sin\delta$) on PAV samples at 76 °C.

The trends of PAV samples were almost similar to the trends of RTFO samples. Starting from 58 °C to 70 °C, the $G^*/\sin\delta$ of 1.5%, 4.5% and 7.5% NCA samples were almost the same as the control sample where there was no significance difference between the samples. Meanwhile, the $G^*/\sin\delta$ of the 3% and 6% NCA was lower than that of the control sample. At temperature of 76 °C, prior to failure at 82 °C, the $G^*/\sin\delta$ of the modified samples was lower than that of the control sample (Fig. 12). Thus, these results showed that NCA was able to retard the aging process and have high resistance to rutting and fatigue cracking.

4. Conclusions

The sizes of ground charcoal were determined through PSA and TEM. Through these tests, the 15 h grinding achieved the nanocharcoal ash (NCA) with an average particle size of 57.7 nm. The bitumen modified by micro charcoal (MC) and NCA showed improved physical and rheological properties. However, the NCA-modified bitumen recorded higher rutting performance than other particle sizes. Meanwhile, the highest improvement for the unaged samples was displayed by 6% NCA content. This percentage modification resisted rutting until 70 °C, with a rutting parameter of 1709 Pa prior to failure at 76 °C. In addition, the RTFO and PAV aged samples indicated that 6% NCA was the optimum content that can retard the aging of bitumen. The large surface area of NCA built strong particle forces with the bitumen. Thus, the cohesion of the bitumen increased, consequently increasing the stiffness. It is therefore, the addition of NCA enhanced the performance of conventional bitumen in terms of rutting and fatigue cracking.

Acknowledgement

The financial support provided by Malaysian Ministry of Higher Education and Universiti Teknologi Malaysia in the form of a research grant vote no. Q.J130000.2522.18H05 and Q.J130000.2522.11H76 for this study is highly appreciated.

References

[1] T.W. Brown, E.R. Kandhal, P.S. Roberts, F.L. Kim, Y.R. Lee, D.-Y. Kennedy, Hot Mix Asphalt Materials, Mixture Design and Construction, third ed., NAPA research and education foundation, Lanham, Maryland, USA, 2009.
[2] J. Read, D. Whiteoak, The Shell Bitumen Handbook, fifth ed., Thomas Telford Publishing, London, UK, 2003.
[3] The Asphalt Institute, The Asphalt Handbook, 2007th ed., United States of America, 2007.
[4] N.I.M. Yusoff, A.A.S. Breem, H.N.M. Alattug, A. Hamim, J. Ahmad, The effects of moisture susceptibility and ageing conditions on nano-silica/polymer-modified asphalt mixtures, Constr. Build. Mater. 72 (2014) 139–147.
[5] R. Li, F. Xiao, S. Amirkhanian, Z. You, J. Huang, Developments of nano materials and technologies on asphalt materials – a review, Constr. Build. Mater. 143 (2017) 633–648.
[6] G.L. Hornyak, H.F. Tibbals, J. Dutta, J.J. Moore, Introduction to Nanoscience and Nanotechnology, 2009.
[7] W.J. Steyn, Applications of Nanotechnology in Road Pavement Engineering, in: K. Gopalakrishnan, B. Birgisson, P. Taylor, N. Attoh-Okine (Eds.), Nanotechnology in Civil Infrastructure-A Paradigm Shift, Springer Verlag Berlin Heidelberg, 2011, pp. 49–84.
[8] K. Gopalakrishnan, B. Birgisson, P. Taylor, N.O, Attoh-Okine, Nanotechnology in Civil Infrastructure – A Paradigm Shift, 2011.
[9] W.N.A. Wan Azahar, M. Bujang, R. Putra Jaya, M.R. Hainin, M.M.A. Aziz, N. Ngadi, Application of nanotechnology in asphalt binder: a conspectus and overview, J. Teknol. 14 (2015) 85–89.
[10] M.E. Abdullah, K.A. Zamhari, R. Buhari, N.H.M. Kamaruddin, N. Nayan, M.R. Hainin, N.A. Hassan, R.P. Jaya, N.I.M. Yusoff, A review on the exploration of nanomaterials application in pavement engineering, J. Teknol. 73 (4) (2015) 69–76.
[11] C. Fang, R. Yu, S. Liu, Y. Li, Nanomaterials applied in asphalt modification: a review, J. Mater. Sci. Technol. 29 (7) (2013) 589–594.
[12] M.O. Jamshidi, A. Mohd Hasan, M.R. Yao, H. You, Z. Hamzah, Characterization of the rate of change of rheological properties of nano-modified asphalt, Constr. Build. Mater. 98 (2015) (2015) 437–446.

[13] P. Khattak, M.J. Khattab, A. Rizvi, H.R. Zhang, The impact of carbon nano-fiber modification on asphalt binder rheology, Constr. Build. Mater. 30 (2012) (2012) 257–264.
[14] G.H. Shafabakhsh, O.J. Ani, Experimental investigation of effect of nano TiO_2/SiO_2 modified bitumen on the rutting and fatique performance of asphalt mixtures containing steel slag aggregates, Constr. Build. Mater. 98 (2015) (2015) 692–702.
[15] H. Zhang, C. Zhu, J. Yu, C. Shi, D. Zhang, Influence of surface modification on physical and ultraviolet aging resistance of bitumen containing inorganic nanoparticles, Constr. Build. Mater. 98 (2015) 735–740.
[16] M.W. Hussin, N.H.A.S. Lim, A.R.M. Sam, M. Samadi, M.a. Ismail, N.F. Ariffin, N.H. a. Khalid, M.Z.A. Majid, J. Mirza, H. Lateef, Long term studies on compressive strength of high volume nano palm oil, J. Teknol. 77 (2015) 15–20.
[17] M.Y.Mo hd Ibrahim, P.J. Ramadhansyah, H. Mohd Rosli, M.H. Wan Ibrahim, M. N. Fadzli, Utilization of nano silica as cement paste in mortar and porous concrete pavement, Adv. Mater. Res. 1113 (2015) 135–139.
[18] S. Nikmatin, A. Syafiuddin, A.B.H. Kueh, Y.A. Purwanto, Effects of nanoparticle filler on thermo-physical properties of rattan powder-filled polypropylene composites, J. Teknol. 77 (16) (2015) 181–187.
[19] J. Deng, Y. You, V. Sahajwalla, R.K. Joshi, Transforming waste into carbon-based nanomaterials, Carbon N. Y. 96 (2016) 105–115.
[20] P. Shafigh, H. Bin Mahmud, M.Z. Jumaat, M. Zargar, Agricultural wastes as aggregate in concrete mixtures – a review, Constr. Build. Mater. 53 (2014) 110–117.
[21] K. Gunasekaran, P.S. Kumar, M. Lakshmipathy, Mechanical and bond properties of coconut shell concrete, Constr. Build. Mater. 25 (1) (2011) 92–98.
[22] N. Jeffry, S.N.A. Putra Jaya, R. Manap, N. Miron, N.A. Abdul Hassan, The influence of coconut shell as coarse aggregate in asphalt mixture, Key Eng. Mater. 700 (2016) (2016) 227–237.
[23] Food, and agriculture organization of the united nations (FAOSTAT), Statistics Division, Food and Agriculture Organization of the United Nations Online Available: http://faostat3.fao.org/browse/Q/*/E 2015 Accessed: 01-Jan-2015.
[24] J.E. Sarki, J. Hassan, S.B. Aigbodion, V.S. Oghenevweta, Potential of using coconut shell particle fillers in eco-composite materials, J. Alloys Compd. 509 (5) (2011) 2381–2385.
[25] S. Ouyang, S. Xu, S. Song, N. Jiao, Coconut shell-based carbon adsorbents for ventilation air methane enrichment, Fuel 113 (2013) (2013) 420–425.
[26] S. Zhao, B. Huang, X. Shu, P. Ye, Laboratory investigation of biochar-modified asphalt mixture, Transp. Res. Rec. J. Transp. Res. Board 2445 (2014) (2014) 56–63.
[27] X. Zhao, S. Huang, B. Ye, X.P. Shu, X. Jia, Utilizing bio-char as a bio-modifier for asphalt cement: a sustainable application of bio-fuel by-product, Fuel 133 (10) (2014) 52–62.
[28] A.N. Amirkhanian, F. Xiao, Characterization of unaged asphalt binder modified with carbon nano particles, Int. J. Pavement Res. Technol. 4 (5) (2011) 281–286.
[29] M.M. Jebasingh, G.A. Wilbert, Fabrication and evaluation of nano carbon reinforced polymer composites, Int. J. Res. Eng. Technol. 4 (5) (2015) 147–151.
[30] ASTM D5976, Standard Specification for Type I Polymer Modified Asphalt Cement for Use in Pavement Construction1 no. Reapproved, ASTM International, West Conshohocken, PA, USA, 2000.
[31] ASTM D5, Standard Test Method for Penetration of Bituminous Materials., ASTM International, West Conshohocken, PA, USA, 2013.
[32] ASTM D36, Standard Test Method for Softening Point of Bitumen (Ring-and-Ball Apparatus), ASTM International, West Conshohocken, PA, USA, 2014.
[33] ASTM D4402, D4402M-15, Standard Test Method for Viscosity Determination of Asphalt at Elevated Temperatures Using a Rotational Viscometer 5–7, American Society for Testing and Materials, West Conshohocken, PA, United States, 1999.
[34] ASTM D113-07, Standard Test Method for Ductility of Bituminous Materials. 1–4, ASTM International, West Conshohocken, PA, USA, 2007.
[35] ASTM D7175, Standard Test Method for Determining the Rheological Properties of Asphalt Binder Using a Dynamic Shear Rheometer, ASTM International, West Conshohocken, PA, USA, 2015.
[36] ASTM D2872-12e1, Standard Test Method for Effect of Heat and Air on a Moving Film of Asphalt (Rolling Thin-Film Oven Test) 1–6, ASTM International, West Conshohocken, PA, USA, 2012.
[37] ASTM D6521-13, Standard Practice for Accelerated Aging of Asphalt Binder Using a Pressurized Aging Vessel (PAV) 1–6, ASTM International, West Conshohocken, PA, USA, 2013.
[38] A. Hornyak, G.L. Dutta, J. Tibbals, H.F. Rao, Introduction to Nanoscience, CRC Press, Boca Raton, FL, USA, 2008.
[39] L.G. Austin, P. Bagga, An analysis of fine dry grinding in ball mills, Powder Technol. 28 (1) (1981) 83–90.